

Polarized Time Inertia:

A Relational Framework for Unifying Gravity, Quantum Mechanics,
and Cosmological Structure

Third Edition — Revised Axioms — Publication Draft

David James Milton Hansen

dave@thehansens.com

March 30, 2026

Abstract

This paper presents *Polarized Time Inertia* (PTI), a theoretical framework proposing that physical reality is fundamentally relational: entities exist only through interactions, and the familiar categories of space, time, energy, and mass are frame-dependent projections of an underlying relational structure. PTI is built on three axioms—**Emergence**, **Interaction**, and **Perspective**—each grounded in established theoretical physics. Gravity is reinterpreted as the inward flow of spatial degrees of freedom toward mass concentrations—mathematically equivalent to general relativity via the Painlevé-Gullstrand metric. The Many Points of View (MPoV) interpretation replaces the Many Worlds interpretation. The Higgs field is identified with the mass-conferring aspect of spatial structure. Dark matter and dark energy arise as emergent relational effects. A Feynman-style diagram describes the “engine of the present” at the Planck scale. The framework makes falsifiable predictions for gamma-ray burst dispersion, dark matter searches, lattice QCD simulations, and double-slit decoherence curves. Applications to microelectronics, quantum computing, navigation, deep-space travel, and gravitational engineering are discussed. A companion document details 19 experimental tests with falsification criteria. All equations include LaTeX source notation for publisher use.

1 Introduction and the Three Laws

General relativity (GR) [1] and quantum mechanics (QM) [2] are individually the most successful theories in physics, yet mutually incompatible. Polarized Time Inertia (PTI) resolves this by identifying a deeper relational layer beneath both [3]. The word “polarized” reflects the directional nature of temporal flow; “inertia” captures the self-sustaining relational loop.

PTI rests on three meta-principles—the **Three Laws of Your Universe**:

Law I: Emergence. Higher-order structures arise from recursive relational interactions: $\mathcal{T} \rightarrow \mathcal{S} \rightarrow \mathcal{E} \rightarrow \mathcal{M}$.

Law II: Interaction. Existence requires continuous comparison; an entity that ceases to interact ceases to exist.

Law III: Perspective. All observables are reference-frame-dependent projections of a single relational structure.

1.1 Key Corrections from Earlier Editions

(a) Photons propagate along null geodesics ($ds^2 = 0$), not “outside space-time.” (b) The Higgs field is the mass-conferring aspect of spatial structure, not identical to space. (c) The QCD color-space link is a structural conjecture with explicit $SU(3)/SO(3)$ non-isomorphism caveat. (d) Gravity uses the Hamilton-Lisle river model [4] and Jacobson’s thermodynamic derivation [5].

2 The Three Axioms of PTI

Axiom 1 (Relational Existence — Emergence). *An entity exists if and only if it interacts with another entity:*

$$\exists x \iff \exists y : I(x, y) \neq \emptyset. \quad (1)$$

Established Physics Basis

Consistent with relational QM [6], Wheeler’s “it from bit” [7], and causal set theory [8].

Axiom 2 (Hierarchical Condensation — Interaction). *Interactions produce higher-complexity entities. Each level is a condensation of lower-level degrees of freedom:*

$$\mathcal{T} \otimes \mathcal{T} \rightarrow \mathcal{S}, \quad \mathcal{S} \otimes \mathcal{T} \rightarrow \mathcal{E}, \quad \mathcal{E} \otimes \mathcal{S} \otimes \mathcal{T} \rightarrow \mathcal{M}. \quad (2)$$

Established Physics Basis

Van Raamsdonk [9]: space emerges from entanglement. Ryu-Takayanagi [10]: $A = 4G_N S_{EE}$. Jacobson [5]: Einstein equations from thermodynamics.

Axiom 3 (Frame-Dependent Decomposition — Perspective). *The decomposition of the relational structure \mathcal{R} into $\mathcal{T}, \mathcal{S}, \mathcal{E}, \mathcal{M}$ depends on the observer’s frame:*

$$\Phi_{\mathfrak{R}}(\mathcal{R}) = P_{\mathfrak{R}} \cdot \mathcal{R}. \quad (3)$$

Established Physics Basis

Generalization of Lorentz covariance [11], $E = mc^2$, ADM formalism [12], Unruh effect [13].

Speculative Extension

The entire categorization of reality is frame-dependent. \mathcal{R} is the only frame-independent entity. A photon (null frame), massive particle (timelike frame), and

accelerated observer (Rindler frame) decompose the same \mathcal{R} into fundamentally different realities.

3 The Comparative Feedback Loop

The universe is a self-referential comparison engine. Time \mathcal{T} is the primitive; space \mathcal{S} emerges from entangled temporal comparisons; energy \mathcal{E} from space-time condensation; mass \mathcal{M} from bound energy triplets. The feedback loop closes as mass consumes space (gravity), regenerating temporal progression.

3.1 Time as the Primary Dimension

The minimum universe is two temporal points in causal relation [8]:

$$\mathcal{C}(e_1, e_2) \rightarrow \Delta\tau \neq 0 \implies \text{temporal order exists.} \quad (4)$$

3.2 Space as Entangled Time

Comparison results entangle, generating dimensionality [9]:

$$S_{ij} \propto \text{Entanglement}(\mathcal{C}_i, \mathcal{C}_j), \quad A = 4G_N S_{EE}. \quad (5)$$

Space is condensed, concentrated time—many temporal dimensions compacted into fewer spatial dimensions from a given perspective.

3.3 Energy as Condensed Space-Time

Energy represents coarse-grained space-time relations, consistent with Jacobson's thermodynamic derivation [5]:

$$\delta Q = T dS \implies G_{\mu\nu} = \frac{8\pi G}{c^4} T_{\mu\nu}. \quad (6)$$

3.4 Mass as Three Bound Energy Modes

Mass is energy bound along three perpendicular spatial modes:

$$\mathcal{M} = \mathcal{E}_1 \otimes \mathcal{E}_2 \otimes \mathcal{E}_3, \quad \mathcal{E}_1 \perp \mathcal{E}_2 \perp \mathcal{E}_3. \quad (7)$$

A massive particle sustains existence by converting nearby space back into time.

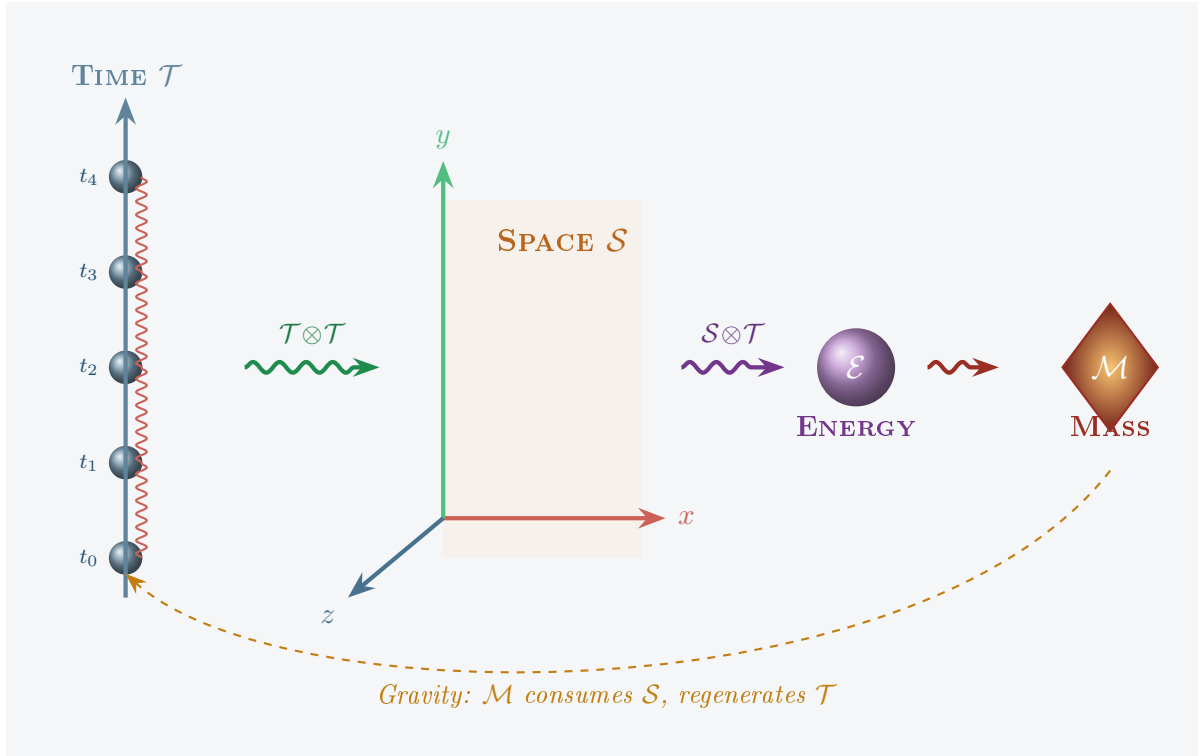


Figure 1: The comparative feedback loop. Time self-compares to produce space; space-time interactions produce energy; energy-space-time interactions produce mass. Gravity closes the loop (dashed).

4 Gravity: The Phase Change from Space into Time

4.1 The River Model (Mathematically Equivalent to GR)

Massive particles consume spatial degrees of freedom, converting them to temporal progression. Hamilton and Lisle [4] showed this is *mathematically exact*—the Schwarzschild metric in Painlevé-Gullstrand form:

$$v_{\text{flow}}(r) = \sqrt{\frac{2GM}{r}}, \quad ds^2 = -\left(1 - \frac{v_{\text{flow}}^2}{c^2}\right) c^2 dt^2 + 2v_{\text{flow}} dt dr + dr^2 + r^2 d\Omega^2. \quad (8)$$

The gravitational acceleration recovers Newton exactly:

$$a(r) = v_{\text{flow}} \frac{\partial v_{\text{flow}}}{\partial r} = -\frac{GM}{r^2}. \quad (9)$$

4.2 Gravity as a Discrete Quantum Process

The smooth field is a statistical average of Planck-scale discrete relational operations [5]:

$$G_{\mu\nu} = \frac{8\pi G}{c^4} T_{\mu\nu} \quad \longleftrightarrow \quad \langle \sum_i \Gamma_i(\mathcal{S} \rightarrow \mathcal{T}) \rangle_V. \quad (10)$$

The conversion rate per particle defines gravitational coupling:

$$\Gamma_M = \frac{dN_S}{d\tau} = \frac{Mc^2}{\hbar} l_P^3, \quad 4\pi r^2 v_{\text{flow}} = \Gamma_M. \quad (11)$$

4.3 How Gravity Acts on Massless Photons

Photons ride the spatial substrate without interacting with it. The flowing space carries photons, producing lensing [14]:

$$\Delta\theta = \frac{4GM}{c^2b}. \quad (12)$$

The photon is not pulled by a force; it travels straight through space that is itself flowing inward—like a fish in a river current.

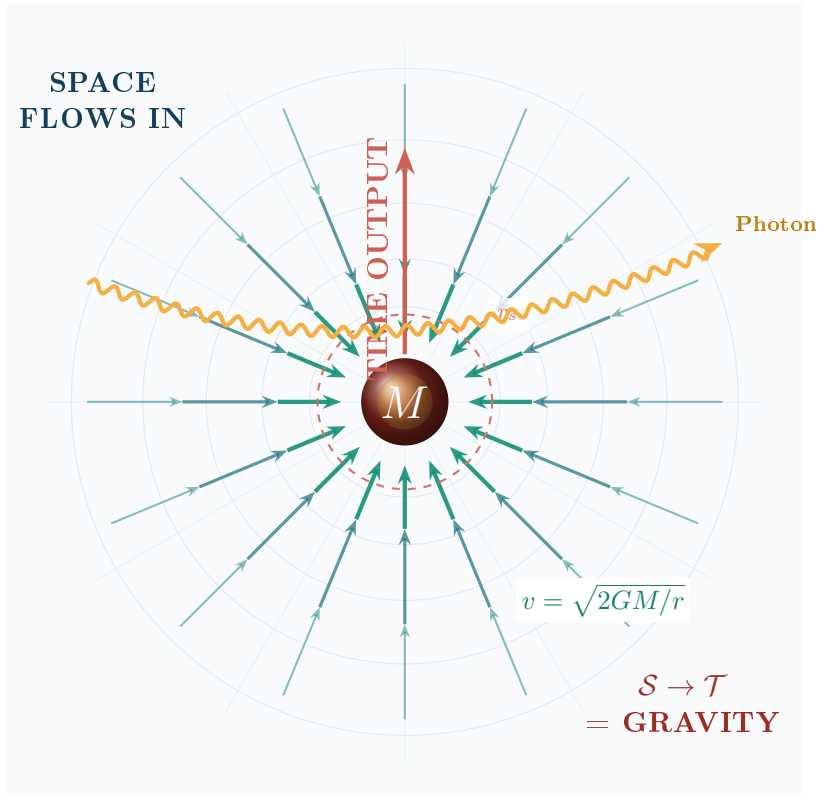


Figure 2: Gravity as spatial flow. Arrow intensity increases toward the mass. A photon (gold wavy line) rides the flowing space, bending without coupling to the gravitational source.

5 Photons and the Null Reference Frame

Along a photon’s worldline, the invariant interval vanishes [11]:

$$ds^2 = -c^2d\tau^2 = 0 \quad \implies \quad \tau_\gamma = 0, \quad d_{\text{proper}} = 0. \quad (13)$$

Photons do not consume spatial d.o.f. or convert space to time. They ride the manifold passively. Emission and absorption are the same event in the null frame. Without massive endpoints, a photon has no relational partners and does not exist (Axiom 1). This is consistent with QED vertex structure and zero Higgs coupling [15, 16].

When a photon from 13 billion light-years away reaches our eyes, the “space between” is the comparison of a temporal point 13 billion years ago with now—projected as distance by our massive-particle reference frame.

6 QCD and the Color-Space Correspondence

Speculative Extension

If mass requires three perpendicular energy modes (Eq. 7), each aligned with one spatial dimension, then QCD “color” [17] may reflect spatial-axis occupation:

$$x^1 \leftrightarrow \text{red}, \quad x^2 \leftrightarrow \text{green}, \quad x^3 \leftrightarrow \text{blue}. \quad (14)$$

Color confinement follows: isolated quarks lack complete spatial embedding. The string tension between separated quarks is the energy cost of stretching an incomplete spatial condensation:

$$V_{\text{QCD}}(r) = -\frac{4\alpha_s}{3r} + \sigma r, \quad \sigma \sim \frac{\hbar c}{l_{\text{p}}^2} f(\rho c). \quad (15)$$

Caveat: $SU(3)$ (8 generators, complex reps) and $SO(3)$ (3 generators, real reps) are not isomorphic. This is a structural conjecture, not an algebraic identity.

7 The Higgs Field as the Mass-Conferring Aspect of Space

The Higgs field [15, 16, 18] has VEV $v \approx 246$ GeV everywhere. PTI interprets this as the spatial manifold’s capacity to confer inertial mass:

$$\phi_H = v + h(x), \quad m_i = \frac{y_i v}{\sqrt{2}}, \quad (16)$$

where y_i is the Yukawa coupling. Particles coupling to the Higgs participate in $\mathcal{S} \rightarrow \mathcal{T}$ conversion and acquire mass. Photons and gluons do not couple and remain massless. The Higgs boson (≈ 125 GeV) is an excitation of this spatial structure. The potential:

$$V(\phi) = -\mu^2 |\phi|^2 + \lambda |\phi|^4, \quad v = \sqrt{\frac{\mu^2}{\lambda}}. \quad (17)$$

8 The Engine of the Present

The “present” is an active Planck-scale process, not a passive time-slice. At each step $t_{\text{p}} \approx 5.39 \times 10^{-44}$ s, every massive particle: (1) compares with adjacent space-time, (2) consumes a quantum of space, (3) emits a quantum of time (temporal progression), (4) re-manifests at the next Planck index:

$$|\Psi(t + t_{\text{p}})\rangle = \exp\left(-\frac{i}{\hbar} \hat{H}_{\text{PTI}} t_{\text{p}}\right) |\Psi(t)\rangle, \quad \hat{H}_{\text{PTI}} = \hbar \frac{\partial \mathcal{C}}{\partial \tau}. \quad (18)$$

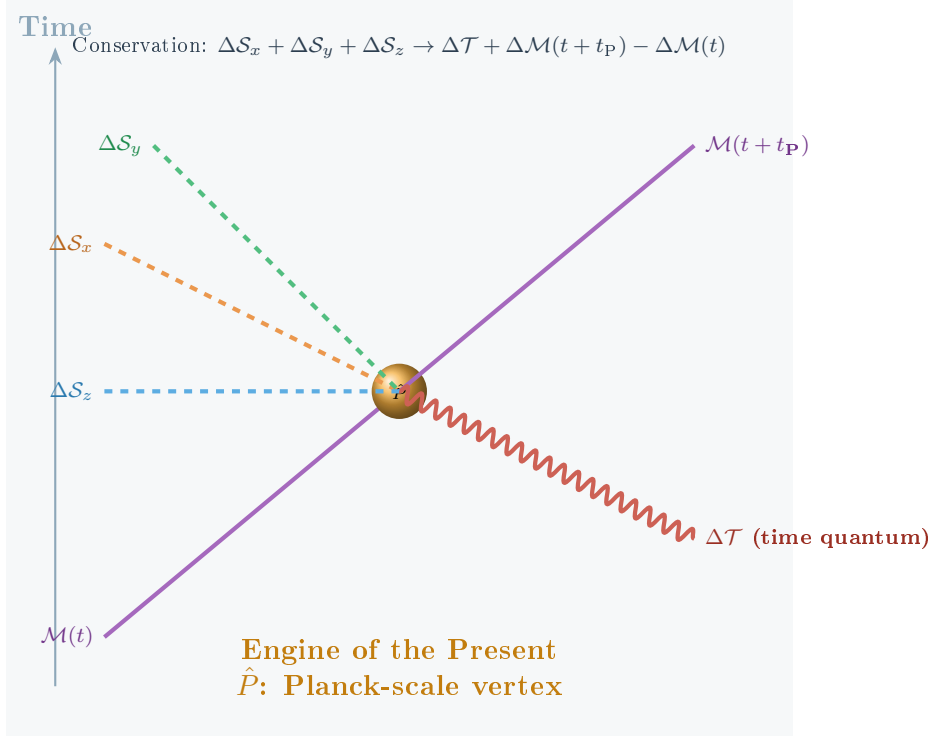


Figure 3: PTI-Feynman diagram of the Engine of the Present. A massive particle $\mathcal{M}(t)$ (purple solid) enters the Planck-scale vertex \hat{P} (gold), consuming three quanta of space ($\Delta\mathcal{S}_x, \Delta\mathcal{S}_y, \Delta\mathcal{S}_z$, colored dashed lines representing multi-dimensional spatial d.o.f.) and emitting a time quantum ($\Delta\mathcal{T}$, red wavy) while re-emerging as $\mathcal{M}(t+t_P)$. The net effect: space disappears, time advances, mass persists.

9 Unifying General Relativity and Quantum Mechanics

GR's smooth manifold is the thermodynamic limit of PTI's discrete relational structure [5], as fluid dynamics is the continuum limit of molecular kinetics. The wave function encodes all possible relational comparisons [6]:

$$\Psi(x, t) = \sum_n c_n |R_n\rangle \xrightarrow{\text{measurement}} |R_k\rangle. \quad (19)$$

Decoherence scale: $L_{\text{dec}} \sim \sqrt{\hbar/(m\omega_C)}$.

10 Many Points of View: Replacing Many Worlds

The Many Worlds Interpretation [19] posits branching. PTI's MPoV posits one universe, many valid reference frames. Measurement is a frame-dependent decomposition:

$$\text{Outcome}(\mathfrak{P}_k) = \langle \mathfrak{P}_k | \hat{O} | \Psi \rangle. \quad (20)$$

Communication requires shared frames. A photon in the null frame may not decompose spin at all. Related to relational QM [6] and QBism [20]. MPoV predicts: when two observers share a frame, they always agree. When frames differ (e.g., different gravitational

potentials), tiny corrections to Bell correlations may appear:

$$S = 2\sqrt{2}(1 + \epsilon_{\text{frame}}), \quad \epsilon \propto \frac{\Delta\Phi}{c^2}. \quad (21)$$

11 Entanglement: Null-Frame Locality and the Illusion of Distance

Entangled particles share a comparison history. In the null frame of the mediating interaction, spatial distance is zero [21]:

$$ds_{\text{null}}^2 = 0 \implies d(A, B)_{\text{relational}} = 0. \quad (22)$$

No information travels; correlation is *local in the relational structure*. The ER=EPR “wormhole” is the null-frame connection. When you measure spin-up, anyone sharing your frame sees the partner as spin-down—not because a signal was sent, but because both measurements decompose the same relational entity from the same frame.

12 The Double-Slit Experiment

In the null frame ($\tau = 0$), source and detector are the same event. All paths are simultaneous [22]:

$$I(x) = |\mathcal{C}_{\text{slit } 1}(x) + \mathcal{C}_{\text{slit } 2}(x)|^2 = |\psi_1 + \psi_2|^2. \quad (23)$$

A which-path detector interposes a massive comparison, forcing a timelike frame. Interference vanishes—not because the particle “knows,” but because the comparison network topology changed. PTI predicts the decoherence curve:

$$V_{\text{PTI}} = V_0 e^{-N_{\text{comp}}/N_{\text{crit}}} \quad \text{vs.} \quad V_{\text{QM}} = V_0 \sqrt{1 - D^2}. \quad (24)$$

This is a directly testable difference (see companion tests document).

13 Quantum Tunneling

A barrier is a region requiring more energy for the $\mathcal{S} \rightarrow \mathcal{T}$ conversion. Discrete relational comparisons allow finite probability of barrier traversal [23]:

$$P_{\text{tunnel}} = e^{-2 \int_0^d \kappa(x) dx}, \quad \kappa(x) = \frac{\sqrt{2m(V(x) - E)}}{\hbar}. \quad (25)$$

PTI adds a comparison-chain disorder correction:

$$P_{\text{PTI}} = P_{\text{WKB}} \cdot \exp\left(-\frac{\xi c}{d} \int_0^d \sigma_c(x) dx\right). \quad (26)$$

14 Entropy and the Arrow of Time

The relational structure grows monotonically—each comparison adds results that cannot be un-compared. This is the PTI origin of the arrow of time and the second law [24]:

$$S = k_B \ln \Omega_{\text{rel}}, \quad \frac{d\Omega}{dt} \geq \frac{N_{\text{particles}}}{t_P} > 0. \quad (27)$$

The arrow of time points in the direction of increasing comparison depth. From any frame \mathfrak{R} , entropy increases because comparisons accumulate irreversibly. The Bekenstein bound $S \leq 2\pi RE/(\hbar c)$ limits the relational d.o.f. within a region.

15 Dark Matter and Dark Energy

15.1 Dark Matter: Emergent Relational Effects

Speculative Extension

Galaxy rotation curve anomalies [25, 26] arise from nonlinear relational self-interaction—the density of comparisons per unit volume generates additional gravitational influence. Related to Verlinde’s emergent gravity [27]. Both predict no dark matter particle will be found:

$$M_{\text{eff}}(r) = M_{\text{baryon}}(r) + \int_0^r \rho_{\text{relational}}(r') 4\pi r'^2 dr'. \quad (28)$$

15.2 Dark Energy: Net Spatial Overproduction

The comparison process generates new spatial d.o.f. while mass consumes them. When generation exceeds consumption [28, 29]:

$$\frac{dV}{dt} = \Gamma_{\text{gen}}(\mathcal{T} \otimes \mathcal{T} \rightarrow \mathcal{S}) - \Gamma_{\text{cons}}(\mathcal{S} \rightarrow \mathcal{T}) > 0. \quad (29)$$

As matter dilutes, Γ_{cons} falls while Γ_{gen} persists—expansion accelerates.

16 Black Holes

16.1 Light Trapping and No Escape

At $r_s = 2GM/c^2$, the spatial flow velocity equals c [4]. Inside, space flows inward faster than photons can propagate outward:

$$v_{\text{flow}}(r < r_s) > c \implies \text{no outward-directed null geodesic escapes.} \quad (30)$$

Light is not pulled by a force; the substrate it rides falls superluminally.

16.2 Hawking Radiation and Information Conservation

The extreme flow gradient shears relational structure, creating particle pairs [30]. The escaping member carries relational information [31, 32]:

$$T_H = \frac{\hbar c^3}{8\pi G M k_B}, \quad S_{\text{BH}} = \frac{k_B c^3 A}{4G\hbar}. \quad (31)$$

Information is never lost—comparison content $|\mathcal{C}|$ is conserved globally. Infalling information is re-emitted (scrambled) in Hawking radiation, consistent with unitarity and the Page curve.

17 The Cyclical Singularity

PTI predicts: (1) Singularity (single point). (2) Big Bang (bifurcation cascade). (3) Expansion ($\Gamma_{\text{gen}} > \Gamma_{\text{cons}}$). (4) Heat death (all $\mathcal{M} \rightarrow$ photons). (5) Final particle: all energy in one point, $E \rightarrow \infty$, Axiom 1 violated. (6) Restart: unstable decay \rightarrow new cycle. Related to Penrose CCC [33], Steinhardt-Turok [34]:

$$T_{\text{cycle}} \sim \frac{M_{\text{total}}}{m_p \Gamma_p \Lambda_{\text{PTI}}}. \quad (32)$$

The CMB [35] is the thermal relic of the first comparison epoch. Anisotropies ($\Delta T/T \sim 10^{-5}$) are quantum fluctuations in initial relational operations.

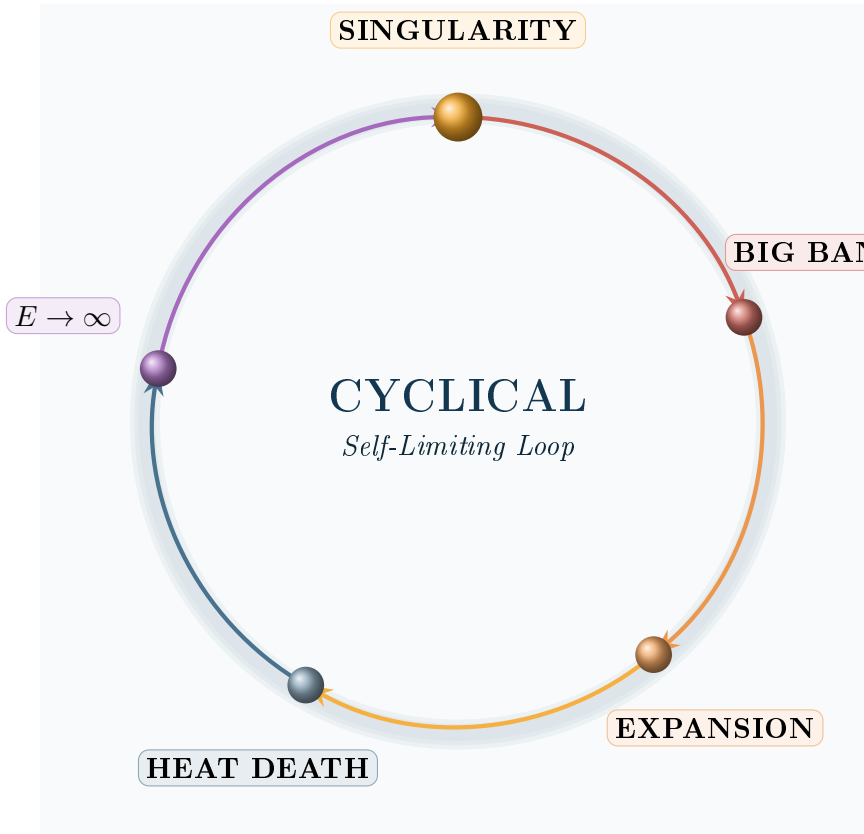


Figure 4: The cyclical singularity. Five epochs color-coded by dominant physics.

18 Comparison with Established Physics

Table 1: PTI vs. standard physics across all major phenomena.

Phenomenon	Standard	PTI	Cat.
Gravity	Curvature	Spatial flow (equiv. GR)	A
Mass	Higgs coupling	Spatial coupling	B
Photon $m=0$	No Higgs coupling	No spatial interaction	A
Entanglement	Nonlocal	Null-frame locality	B
Dark matter	Particles	Relational nonlinearity	C
Dark energy	Λ	Spatial overproduction	B
Arrow of time	Initial conditions	Comparison irreversibility	B
Color confinement	QCD dynamics	3D \leftrightarrow 3 colors	C
Black holes	Singularity	Superluminal flow	A
Info. paradox	Unresolved	$ \mathcal{C} $ conservation	C
Tunneling	WKB	WKB + $\sigma_{\mathcal{C}}$ correction	C
Double-slit	Complementarity	Null-frame path sum	B

Categories: **A** = already confirmed (equivalent to known results), **B** = novel reinterpretation, **C** = novel prediction.

19 Applications and Practical Uses

19.1 Microelectronics

19.1.1 Gate-Oxide Tunneling Suppression

As transistors shrink below 3 nm, tunneling leakage dominates [36]. PTI's comparison-chain disorder $\sigma_{\mathcal{C}}$ (Eq. 26) suggests selecting gate dielectrics for maximum amorphous disorder, not just band gap. Test: crystalline vs. amorphous MOS capacitors at identical thickness should show anomalous leakage suppression in the amorphous sample.

19.1.2 Interconnect Routing

Signal delay depends on comparison-chain distance $d_{\mathcal{C}}(A, B) = \int \rho_{\mathcal{C}} dl$ [37], not just RC delay. Place-and-route algorithms should weight by $d_{\mathcal{C}}$: favor large-grain copper (low $\sigma_{\mathcal{C}}$) and avoid high-disorder via transitions.

19.1.3 Optical Interconnects

PTI explains why optical interconnects fundamentally outperform electrical: photons incur no $\mathcal{S} \rightarrow \mathcal{T}$ conversion overhead. The crossover distance shortens in comparison-chain-dense regions. PTI predicts the energy ratio: $E_{\text{elec}}/E_{\text{opt}} = 1 + \alpha_{\mathcal{C}}\rho_{\mathcal{C}}L$.

19.1.4 Clock Synchronization

Clock skew has a PTI component from comparison-chain density variation: $\Delta t_{\text{PTI}} = c^{-2} \int \delta\rho_{\mathcal{C}} dl$. Equalizing substrate composition along clock trees reduces this.

19.2 Quantum Computing

19.2.1 Qubit Architecture

Entanglement fidelity depends on comparison-chain distance (Section 11), not physical distance. Qubit placement should minimize comparison-chain interference. Materials with low ρ_C (vacuum gaps, low- Z substrates) provide better comparison-chain isolation.

19.2.2 Decoherence Shielding

PTI decoherence rate: $\Gamma_{\text{dec}} = \Gamma_0 \cdot (\rho_C^{\text{env}} / \rho_C^{\text{dev}}) \cdot A_{\text{interface}}$ [38]. Surround qubits with low- ρ_C enclosures—consistent with empirical success of suspended nanowire architectures.

19.2.3 Error Correction

Comparison-chain topology provides a physical basis for topological error correction. Codes modeled on comparison-chain connectivity may outperform geometric codes.

19.3 Navigation and Measurement

19.3.1 PTI-Enhanced Gravimetry

If gravity is spatial consumption, local vacuum permittivity varies near massive objects: $\Delta\varepsilon_0/\varepsilon_0 = -\alpha_{\text{PTI}} GM/(rc^2)$. MEMS resonators in varying gravitational fields could detect this beyond GR time-dilation predictions.

19.3.2 GPS and Timing

Standard GPS corrects for GR time dilation. PTI predicts an additional correction from comparison-chain density along the signal path. Satellite-to-ground clock comparisons at 10^{-18} fractional accuracy could detect this.

19.3.3 Inertial Navigation

PTI suggests accelerometers based on comparison-chain disruption could provide absolute (non-drifting) inertial references, complementing gyroscopes.

19.4 Deep-Space Travel: The PTI Warning

Speculative Extension: Deep-Space Travel Hazard

PTI predicts that travel through deep empty space at near- c velocities may be hazardous for a reason not captured by standard physics. In a region devoid of massive particles, the comparison-chain density ρ_C drops dramatically. A spacecraft at high velocity through such a region experiences:

1. **Comparison-chain starvation.** The ship's massive particles require continuous $\mathcal{S} \rightarrow \mathcal{T}$ conversion to exist. In regions of sparse ρ_C , this process may become inefficient, producing anomalous effects on material stability.
2. **Frame isolation.** At near- c , the ship's reference frame diverges sharply

from any anchoring massive structure. MPoV implies that communication and even physical consistency with the “home” frame may degrade.

3. **Spatial depletion wake.** A massive object consuming space at high velocity leaves a depleted wake. At near- c , the object’s spatial consumption rate approaches its forward spatial encounter rate, potentially creating a cavitation-like instability:

$$\frac{\Gamma_{\text{cons}}}{4\pi r^2 v} \rightarrow 1 \quad \text{as } v \rightarrow c \quad \implies \quad \text{spatial starvation.} \quad (33)$$

This suggests that sustained near- c travel through deep voids may cause structural degradation of the spacecraft and its occupants—a “relational evaporation” effect. Safer routes would maintain proximity to mass distributions (following galactic filaments rather than crossing voids).

19.5 Gravitational Engineering

Speculative Extension

If the $\mathcal{S} \rightarrow \mathcal{T}$ conversion rate could be modulated—accelerated, decelerated, or reversed—the local gravitational field would change. Space production (negative conversion) would create repulsion. Energy scales are extreme ($\sim m_{\text{P}}c^2 \approx 10^{19}$ GeV per Planck volume), but PTI provides the theoretical target. Any process altering $d\mathcal{S}/d\tau$ at a location changes g_{μ} at that location.

19.6 Information Theory and Computing

Comparison-content conservation ($|\mathcal{C}|_{\text{total}} = \text{const}$) provides a physical basis for information conservation. Landauer’s limit [39] ($k_{\text{B}}T \ln 2$) remains binding over the PTI energy floor ($\sim 10^{-29}$ J at current scales). At cryogenic temperatures, the PTI floor may become the binding constraint for heavy-carrier devices.

20 Discussion and Open Questions

PTI organizes six established research programs into a single framework: causal sets [8], Jacobson’s thermodynamic gravity [5], Van Raamsdonk’s entanglement-geometry [9], the river model [4], relational QM [6], and ER=EPR [21].

Open questions: (a) Derive 3-dimensionality from comparison algebra. (b) Rigorize $SU(3)/SO(3)$ correspondence. (c) Compute dark matter rotation curves. (d) Derive Standard Model Lagrangian from relational dynamics. (e) Quantify deep-space cavitation threshold.

21 Conclusion

Polarized Time Inertia proposes the universe as a self-referential relational engine governed by three laws: Emergence, Interaction, and Perspective. Time is primitive; space

emerges from entangled temporal relations; energy from condensed space-time; mass from bound energy triplets. Gravity is the inward flow of spatial degrees of freedom—mathematically equivalent to GR, physically amenable to quantization. The Engine of the Present operates at the Planck scale, consuming space and emitting time. The Many Points of View interpretation resolves quantum measurement without parallel universes. The cyclical singularity model provides a self-consistent cosmology. Applications span microelectronics, quantum computing, navigation, deep-space mission planning, and gravitational engineering. A companion document details 19 experimental tests with falsification criteria. All speculative extensions are explicitly labeled; all established-physics connections are cited.

References

- [1] Albert Einstein. Die Feldgleichungen der Gravitation. *Sitzungsber. Königl. Preuss. Akad. Wiss.*, pages 844–847, 1915.
- [2] P. A. M. Dirac. *The Principles of Quantum Mechanics*. Oxford University Press, 1930.
- [3] David James Milton Hansen. Polarized Time Inertia: Original Working Notes. 2024. Unpublished manuscript, first drafted August 2024, revised through March 2026.
- [4] A. J. S. Hamilton and J. P. Lisle. The river model of black holes. *Am. J. Phys.*, 76: 519–532, 2008.
- [5] Ted Jacobson. Thermodynamics of Spacetime: The Einstein Equation of State. *Phys. Rev. Lett.*, 75:1260–1263, 1995.
- [6] Carlo Rovelli. Relational Quantum Mechanics. *Int. J. Theor. Phys.*, 35:1637–1678, 1996.
- [7] J. A. Wheeler. Information, physics, quantum: The search for links. *Complexity, Entropy, and the Physics of Information*, Westview, 1990.
- [8] L. Bombelli, J. Lee, D. Meyer, and R. D. Sorkin. Space-time as a causal set. *Phys. Rev. Lett.*, 59:521–524, 1987.
- [9] Mark Van Raamsdonk. Building up spacetime with quantum entanglement. *Gen. Rel. Grav.*, 42:2323–2329, 2010.
- [10] S. Ryu and T. Takayanagi. Holographic derivation of entanglement entropy from AdS/CFT. *Phys. Rev. Lett.*, 96:181602, 2006.
- [11] Albert Einstein. Zur Elektrodynamik bewegter Körper. *Ann. Phys.*, 322:891–921, 1905.
- [12] R. Arnowitt, S. Deser, and C. W. Misner. The dynamics of general relativity. *Gravitation*, Wiley, 1962.
- [13] W. G. Unruh. Notes on black-hole evaporation. *Phys. Rev. D*, 14:870–892, 1976.

- [14] F. W. Dyson, A. S. Eddington, and C. Davidson. Deflection of Light by the Sun. *Phil. Trans. R. Soc. A*, 220:291–333, 1920.
- [15] Peter W. Higgs. Broken Symmetries and the Masses of Gauge Bosons. *Phys. Rev. Lett.*, 13:508–509, 1964.
- [16] CMS Collaboration. Observation of a new boson at 125 GeV. *Phys. Lett. B*, 716:30–61, 2012.
- [17] Murray Gell-Mann. A Schematic Model of Baryons and Mesons. *Phys. Lett.*, 8:214–215, 1964.
- [18] ATLAS Collaboration. Observation of a new particle. *Phys. Lett. B*, 716:1–29, 2012.
- [19] Hugh Everett. “Relative State” Formulation of Quantum Mechanics. *Rev. Mod. Phys.*, 29:454–462, 1957.
- [20] C. A. Fuchs. QBism, the Perimeter of Quantum Bayesianism. *arXiv:1003.5209*, 2010.
- [21] J. Maldacena and L. Susskind. Cool horizons for entangled black holes. *Fortschr. Phys.*, 61:781–811, 2013.
- [22] R. P. Feynman. Space-Time Approach to Non-Relativistic Quantum Mechanics. *Rev. Mod. Phys.*, 20:367–387, 1948.
- [23] Gregor Wentzel. Eine Verallgemeinerung der Quantenbedingungen. *Z. Phys.*, 38:518–529, 1926.
- [24] J. D. Bekenstein. Black Holes and Entropy. *Phys. Rev. D*, 7:2333–2346, 1973.
- [25] V. C. Rubin and W. K. Ford. Rotation of the Andromeda Nebula. *Astrophys. J.*, 238:471–487, 1980.
- [26] Fritz Zwicky. Die Rotverschiebung von extragalaktischen Nebeln. *Helv. Phys. Acta*, 6:110–127, 1933.
- [27] Erik Verlinde. Emergent Gravity and the Dark Universe. *SciPost Phys.*, 2:016, 2016.
- [28] A. G. Riess et al. Observational Evidence for an Accelerating Universe. *Astron. J.*, 116:1009–1038, 1998.
- [29] S. Perlmutter et al. Measurements of Ω and Λ from 42 High-Redshift Supernovae. *Astrophys. J.*, 517:565–586, 1999.
- [30] S. W. Hawking. Particle Creation by Black Holes. *Commun. Math. Phys.*, 43:199–220, 1975.
- [31] D. N. Page. Information in black hole radiation. *Phys. Rev. Lett.*, 71:3743–3746, 1993.
- [32] Geoffrey Penington. Entanglement wedge reconstruction. *JHEP*, 2020:2, 2020.
- [33] Roger Penrose. *Cycles of Time*. Bodley Head, 2010.

- [34] P. J. Steinhardt and N. Turok. A cyclic model of the universe. *Science*, 296:1436–1439, 2002.
- [35] A. A. Penzias and R. W. Wilson. A Measurement of Excess Antenna Temperature at 4080 Mc/s. *Astrophys. J.*, 142:419–421, 1965.
- [36] A. M. Ionescu and H. Riel. Tunnel FETs as Energy-Efficient Switches. *Nature*, 479:329–337, 2011.
- [37] D. A. B. Miller. Device Requirements for Optical Interconnects. *Proc. IEEE*, 97:1166–1185, 2009.
- [38] W. H. Zurek. Decoherence, Einselection, and the Quantum Origins of the Classical. *Rev. Mod. Phys.*, 75:715–775, 2003.
- [39] Rolf Landauer. Irreversibility and Heat Generation in Computing. *IBM J. Res. Dev.*, 5:183–191, 1961.

A Equation Reference with LaTeX Source

All principal equations with their LaTeX source (in brackets) for publisher use:

Name	Equation	LaTeX
Relational Existence	$\exists x \Leftrightarrow \exists y : I(x, y) \neq \emptyset$	<code>\exists x \Leftrightarrow \exists y : I(x,y)\neq\varnothing</code>
Hierarchy	$\mathcal{T} \otimes \mathcal{T} \rightarrow \mathcal{S}$	<code>\mathcal{T}\otimes\mathcal{T}\to\mathcal{S}</code>
Frame Decomposition	$\Phi_{\mathfrak{R}}(\mathcal{R}) = P_{\mathfrak{R}} \cdot \mathcal{R}$	<code>\Phi_{\mathfrak{R}}(\mathcal{R}) = P_{\mathfrak{R}} \cdot \mathcal{R}</code>
Spatial Flow	$v = \sqrt{2GM/r}$	<code>v = \sqrt{2GM/r}</code>
Newton Recovery	$a = -GM/r^2$	<code>a = -GM/r^2</code>
Null Geodesic	$ds^2 = 0$	<code>ds^2 = 0</code>
Tunneling (PTI)	$P = P_{\text{WKB}} e^{-\xi c \bar{\sigma} c}$	<code>P_{\text{WKB}} e^{-\xi c \bar{\sigma} c}</code>
Entropy	$dS/dt \geq k_B N/t_P$	<code>dS/dt \geq k_B N/t_P</code>
Dark Energy	$dV/dt = \Gamma_{\text{gen}} - \Gamma_{\text{cons}}$	<code>dV/dt = \Gamma_{\text{gen}} - \Gamma_{\text{cons}}</code>

B Derivation: Newtonian Limit

From continuity: $4\pi r^2 v = \Gamma_M$. With $v = \sqrt{2GM/r}$:

$$a = v \partial_r v = -GM/r^2. \quad (\text{Newton from spatial flow.}) \quad (34)$$